Amplified Spontaneous Emission and Carrier Pinning in Laser Diodes

Shun Lien Chuang, *Senior Member, IEEE*, James O'Gorman, and A. F. J. Levi

Abstract—**Theoretical and experimental results for the temperature dependence of amplified spontaneous emission (ASE) in laser diodes (LD's) and light-emitting diodes (LED's) are presented. Our theoretical model takes into account conduction band nonparabolicity and band-gap renormalization. The gain spectrum is calculated from the theoretical spontaneous emission spectrum and both compare very well with experimental data. From a fit to the observed temperature dependence of ASE for a LED and the gain spectrum for a LD with an identical structure as the LED except for mirror reflectivity we are able to establish carrier density as a function of injection current for both devices. We show that photons fluctuating into cavity modes give rise to substantial subthreshold carrier pinning in laser diodes. These fluctuations extract an extra current from the device and play an increasingly important role with increasing temperature.**

I. Introduction

UNDERSTANDING the physical origin of the temperature dependence of laser diodes is an outstanding problem [1], [2]. For example, threshold current typically increases rapidly at elevated temperatures. In recent years significant effort has been expended with the aim of reducing threshold current by using quantum-well structures [3] or strained materials. It was also hoped that such an approach would reduce the temperature sensitivity of threshold current in laser diodes. Despite much work, the temperature dependence of threshold current, as parameterized by a characteristic activation temperature T_0 has remained essentially unchanged. Why this should be so has not yet been satisfactorily explained.

Recently, we approached the problem from a perspective which highlighted the importance of photon statistics near laser threshold. We were able to show experimentally that fluctuations of photons into cavity modes of a laser diode at subthreshold current contribute to the temperature dependence of the device [4]. In addition, and contrary to popular belief, it has been shown that Auger recombination does not play a dominant role in determining the temperature dependence of threshold current in long wavelength (1.3 μm) laser diodes [5]–[7].

Of course, if one is to successfully model the temperature dependence of laser diodes, then it is important to understand the photon amplification mechanism in the device. Gain spectra have been calculated previously for bulk semiconductors [8]–[10] and quantum-well structures [11]–[15]. The calculation of gain in bulk materials usually involves parabolic band structures since they provide analytical results in the limit of zero scattering linewidth and, therefore, a clear physical picture of the gain process. Inclusion of finite scattering linewidth within a parabolic band structure model has also been applied to the study of gain in bulk and quantum-well semiconductor lasers [11]. In the case of quantum-well lasers, it has been shown that valence-band mixing effects play an important role in determining the gain spectrum [12]–[14]. The situation is somewhat more complicated for strained quantum-well lasers. In these circumstances, the valence-band structure is best described by a Luttinger–Kohn Hamiltonian including the Pikus–Bir strain term resulting in strong mixing between heavy-hole and light-hole bands. In addition to the above, many-body effects, such as the influence of band-gap renormalization and screened excitons, all play important roles in determining gain in semiconductor lasers [15]–[18].

In this paper, we investigate the relationship between carrier pinning and photon emission from index guided edge-emitting laser diodes (LD's) and light-emitting diodes (LED's) at different temperatures. Our theoretical model takes account of conduction band nonparabolicity effects and a carrier dependent band-gap renormalization. Gain spectra are calculated from spontaneous emission spectra using a relationship between the two spectra [19]. Our model preserves the simplicity of the density-matrix formulation and, unlike the conventional approach, satisfies the thermodynamic requirement that the transparency energy occur at the difference of electron and hole chemical potential. An unphysical sign change from gain to absorption below the bandgap assuming a constant linewidth in the conventional model, as pointed out in [20] and [21], does not occur in our model.

Our experiments [22] make use of the fact that spontaneous emission experiences amplification while propagating along the waveguide [23]–[25]. In contrast, nonguided light, which is measured by collecting emission through a window in the substrate, does not experience

Manuscript received September 28, 1992; revised February 5, 1993. The work at the University of Illinois was supported by the Office of Naval Research under Grant N0014-90-J-1821.

S. L. Chuang is with the Department of Electrical and Computer Engineering, University of Illinois, Urbana, Illinois 61801.

J. O'Gorman is with Optronics Ireland, Trinity College, Dublin.

A. F. J. Levi is with the Department of Electrical Engineering and Electrophysics, University of Southern California, Los Angeles, CA 90089-1112.

IEEE Log Number 9209117.

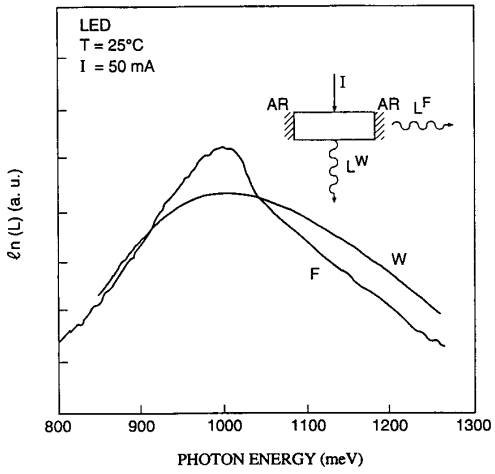

Fig. 1. Measured spontaneous emission spectrum obtained by collecting photons through a window in the substrate L^W and the amplified spontaneous emission spectrum obtained by collecting photons from the facet L^F of a LED.

gain. In Fig. 1, we show the measured window spontaneous emission spectrum L^W of an edge emitting LED. This consists of light collected through the substrate and corrected for free-carrier absorption in the n-type substrate. The amplified spontaneous emission spectrum L^F is also shown. The difference between the two spectra indicates clearly the effect of amplification for spontaneous emission light traveling along the waveguide. By comparing the measured emission spectra L^F and L^W we extract the carrier density n for various drive currents I and temperatures T. Both TE and TM polarizations of the facet light are considered, while the window light has no dependence on polarization. Using the same device structure, but introducing facet mirrors to form a laser cavity, we then measure the gain spectrum for the LD. We use a standard bulk active region buried heterostructure design. The active region consists of an InGaAsP layer of thickness $d = 0.14$ μm with a room temperature bandgap of $E_g^0 = 968.4$ meV (wavelength $\lambda_g = 1.28$ μm) lattice matched to an n-type InP substrate and capped by a layer of p-type InP. After a two-step regrowth process, the active region has a width $w = 1$ μm and is surrounded by InP. The device is cleaved to a length $l = 260$ μm and bonded p-side down onto a BeO submount. LD's are as cleaved devices and LED's are formed by antireflection coating both facets. A gap or window in the metalization making electrical contact to the back of the n-type InP substrate allows collection of nonguided light emitted from the active region.

From a fit of the calculated to measured LED and LD gain spectra, we extract carrier density for various drive currents and temperatures. By comparing the relationship between carrier concentration and injection current for LED and LD at two different temperatures, we find substantial carrier pinning for the LD below lasing threshold. This pinning arises due to subthreshold fluctuations into laser cavity modes. These fluctuations, which extract a significant current from the LD, play an increasingly important role with increasing temperature.

In Section II, we present a theoretical model for gain spectra, spontaneous emission and amplified spontaneous emission spectra taking into account conduction band nonparabolicity. Our theory is then used in Section III to compare with experimental results and to extract carrier density at different drive currents and temperatures. We show that our theoretical model agrees very well with experimental data. We then summarize our results in Section IV.

II. Theory

A. Conventional Model for Gain

Conventionally, the optical gain spectrum $g_{conv}(\omega)$ in a semiconductor laser is calculated from the imaginary part of the linear susceptibility $\chi(\omega)$ in the density-matrix formulation [11], [12]

$$g_{conv}(\omega) = -\frac{\omega}{n_g c\epsilon_0} \operatorname{Im} \epsilon_0 \chi(\omega)$$

$$= \frac{\omega}{n_g c\epsilon_0} \frac{2}{V} \sum_k \frac{M_{cv}^2 \gamma_k}{[E_{cv}(k) - \hbar\omega]^2 + \gamma_k^2} \cdot [f_c(k) - f_v(k)] \quad (1)$$

where ω is the optical angular frequency, n_g is the refractive index of the material, c is the speed of light in free space, and ϵ_0 is the permittivity of the free space. The factor 2 accounts for the spins, V is the volume of the crystal, M_{cv} is the electric-dipole moment matrix, $f_c(k)$ and $f_v(k)$ are the Fermi functions for electrons in the conduction band and in the valence band, respectively. Here the linewidth γ_k depends on the scattering processes, and $E_{cv}(k)$ is the energy separation between a conduction band electron and a valence band hole assuming the k-selection rule for interband transitions.

The electric dipole moment M_{cv} may also be written in terms of Kane's parameter [26] $P = -i(\hbar/m_0)\langle S|P_x|X\rangle$, or an equivalent momentum-matrix parameter E_p in units of energy (eV), i.e.,

$$M_{cv} = |\langle \psi_{ck}(\boldsymbol{r})|\hat{\epsilon} \cdot e\boldsymbol{r}|\psi_{vk}(\boldsymbol{r})\rangle|^2_{\text{angular average}} = \frac{e^2P^2}{3E_{cv}^2(k)} \quad (2)$$

where the factor $1/3$ comes from a three-dimensional angular average, and the conjugate relation between the momentum operator $\boldsymbol{p}$ and the position operator $\boldsymbol{r}$,

$$\boldsymbol{p} = \frac{m_0}{i\hbar}[\boldsymbol{r}, H_0] \quad (3)$$

is used to find the relation $|p_{cv}| = |im_0 r_{cv}E_{cv}/h|$. Using $E_p = 2m_0P^2/\hbar^2 = 2p_{cv}^2/m_0$, we obtain

$$g_{conv}(\omega) = \frac{\omega}{n_g c\epsilon_0} \frac{e^2\hbar^2}{3m_0} E_p \int_0^\infty \frac{k^2dk}{2\pi^2} \frac{1}{E_{cv}^2(k)} \cdot \frac{\gamma_k(f_c - f_v)}{[E_{cv}(k) - \hbar\omega]^2 + \gamma_k^2}. \quad (4)$$

Here m_0 is the free-space electron mass and $\hbar$ is Planck's constant h divided by 2π.

B. Gain Calculated from the Spontaneous Emission Spectrum

The spontaneous emission rate, or the number of emitted photons per second per unit volume per unit energy interval, is given by [27]–[29]

$$R_{sp}(\omega) = \frac{8\pi n_g^2(\hbar\omega)^2}{h^3c^2} g_{sp}(\omega) \tag{5}$$

at a photon energy $\hbar\omega$, where $g_{sp}(\omega)$ is conveniently defined to have the same dimension $(1/\text{cm})$ as gain.

$$g_{sp}(\omega) = \frac{\omega}{n_g c\epsilon_0} \frac{e^2\hbar^2}{3m_0} E_p \int_0^\infty \frac{k^2dk}{2\pi^2} \frac{1}{E_{cv}^2(k)} \cdot \frac{\gamma_k f_c(1 - f_v)}{[E_{cv}(k) - \hbar\omega]^2 + \gamma_k^2}. \tag{6}$$

The above expression differs from that for conventional gain $g_{conv}(\omega)$ by the term $f_c(1 - f_v)$ instead of $f_c - f_v$. Here, we choose to calculate gain $g(\omega)$ from the spontaneous emission spectrum using the expression [19]

$$g(\omega) = \hbar \left(\frac{\pi c}{n_g\omega}\right)^2 \{1 - e^{(\hbar\omega - \Delta\mu)/(k_BT)}\} R_{sp}(\omega) \tag{7}$$

where

$$\Delta\mu = E_g' + \mu_n - \mu_p \tag{8}$$

is the separation between electron and hole chemical potential, μ_n and μ_p, respectively, and $R_{sp}(\omega)$ is calculated using (5) and (6). E_g' is the net band gap taking into account carrier-induced band-gap shrinkage,

$$E_g' = E_g^0 - \zeta n^{1/3} \tag{9}$$

where ζ is assumed to be the $In_{0.53}Ga_{0.47}As$ value [30] 2.2×10^{-5} (meV · cm) and n is the electron concentration (in units of $1/\text{cm}^3$) in the active region. The parameter ζ is also taken to be independent of temperature. Obviously, it would be helpful to know more about this parameter for InGaAsP materials. The quasi-Fermi levels μ_n and μ_p are measured from the conduction band edge and the valence band edge, respectively. Both are defined to be positive in the upward direction using the electron energy picture (i.e., $\mu_p > 0$ means the quasi-Fermi level for the holes is above the valence band edge).

Our gain model ensures that the transparency energy, or the transition from gain to absorption, occurs at $\hbar\omega = \Delta\mu$ [18]–[20], which is the renormalized chemical potential difference in a two-band rigid shift model. The model also circumvents the unphysical situation that gain can change sign below the effective band gap when an energy independent linewidth γ_k is used [20]–[21]. Therefore, it preserves the simplicity of the gain model, yet it contains physically significant features such as the renormalized bandgap and the correct behavior of the transparent photon energy at $\Delta\mu$.

In our model, both heavy hole and light hole bands are taken into account. The contribution of the light hole band to the total gain is typically about 10% of that due to the heavy hole band. We have assumed that the carrier concentration is large enough that exciton effects are screened out. Our model can be further improved by not only taking into account screened exciton effects, but also the momentum dependence of linewidth γ_k.

In Fig. 2(a) and (b) we show results of using (7) to calculate gain from the experimentally measured spontaneous emission spectrum. We then compare the result with an experimental determination of gain using the Hakki–Paoli method, as shown in Fig. 2(b). The details of the experiments will be discussed in Section III. Examination of Fig. 2(b) shows excellent agreement between the two methods and verifies the correctness of both our theoretical and experimental approach. This also demonstrates experimentally the internal consistency of our model.

C. Conduction Band Nonparabolicity Effect

Since the conduction band effective mass in InGaAsP is small, with increasing carrier concentration the electron distribution becomes degenerate before the hole distribution does. Assuming no background doping level, conduction band nonparabolicity effects may become important at high injection levels. Using the conduction band dispersion relation [30]

$$\frac{\hbar^2k^2}{2m_e^*} = E(1 + \alpha E) \tag{10}$$

where $E = E_c(k)$ is the electron energy in the conduction band, m_e^* is the electron effective mass and the nonparabolicity parameter α is given by

$$\alpha = \frac{1}{E_g}\left(1 - \frac{m_e^*}{m_0}\right)\left[1 - \frac{E_g\Delta}{3(E_g + \Delta)(E_g + 2\Delta/3)}\right] \tag{11}$$

we obtain

$$n = N_c \frac{2}{\sqrt{\pi}} \int_0^\infty dx \frac{\sqrt{x(1 + \alpha k_BTx)}(1 + 2\alpha k_BTx)}{1 + e^{(x - x_F)}} \tag{12}$$

where

$$N_c = 2\left(\frac{m_e^*k_BT}{2\pi\hbar^2}\right)^{3/2}$$

$$x = E/k_BT$$

and

$$x_F = \mu_n/k_BT. \tag{13}$$

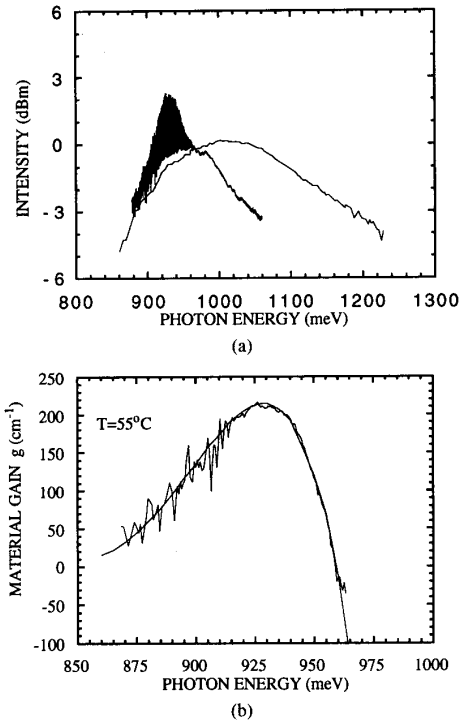

Fig. 2. (a) The Fabry-Perot modulated emission spectrum facet light and the spontaneous emission spectrum window light of a laser diode at T = 55°C and I = 20 mA. (b) Calculated material gain spectrum (solid curve) using the relation (7) from the smoothed data of the spontaneous emission spectrum in (a) and comparison with the measured gain spectrum using the Hakki–Paoli method. The difference in chemical potential is $\Delta\mu$ = 959 meV.

The energy separation $E_{cv}(k)$ in (6) can be obtained from

$$E_{cv}(k) = E_g' + E_c(k) - E_v(k)$$

$$= \begin{cases} E_g^0 - \zeta n^{1/3} + \left[\dfrac{-1 + \sqrt{1 + (2\alpha\hbar^2k^2/m_e^*)}}{2\alpha}\right] \\ \quad + \dfrac{\hbar^2k^2}{2m_h^*} \quad \begin{pmatrix}\text{with conduction band}\\ \text{nonparabolicity}\end{pmatrix} \\ E_g - \zeta n^{1/3} + \dfrac{\hbar^2k^2}{2m_e^*} + \dfrac{\hbar^2k^2}{2m_h^*} \\ \quad \text{(parabolic band model)} \end{cases} \tag{14}$$

where m_h^* equals the heavy-hole effective mass m_{hh}^* for the conduction band to heavy-hole band transitions, and m_h^* equals the light-hole effective mass m_{lh}^* for the conduction band to the light-hole band transitions.

D. Spontaneous Emission (Window Light) and Amplified Spontaneous Emission (Facet Light)

The intensity of window light L^W obtained by collecting spontaneous emission through the substrate, is proportional to the spontaneous emission rate per unit volume per unit energy interval per second multiplied by the energy of each photon and the volume of the active region, wld, i.e.,

$$L^W = \hbar\omega R_{sp}(\omega) wld A^W \exp(-\alpha_{fc} d_s)\, \Delta\epsilon \tag{15}$$

where the area A^W accounts for the window aperture, $\exp(-\alpha_{fc} d_s)$ accounts for free carrier absorption [31] in a substrate of thickness d_s, and $\Delta\epsilon$ is the energy resolution of the spectrometer. The facet light intensity, on the other hand, experiences amplification [24] as the emitted photons travel along the active waveguide region. The expression for LED facet light intensity is

$$L^F = \hbar\omega R_{sp}(\omega) wd \left(\int_0^l e^{g'z}\, dz\right) A^F\, \Delta\epsilon \tag{16}$$

where A^F is the facet aperture function, $g' = \Gamma g$ is the modal gain, and Γ is the optical confinement factor. We find

$$\ln(L^F/L^W) = \ln\left[\frac{e^{g'l} - 1}{g'l}\right] + \ln(A^F/A^W) + \alpha_{fc} d_s. \tag{17}$$

For small d/λ_0 or $(n_g^2 - n_0^2)$, the optical confinement factor for TE polarization can be approximated by [29]

$$\Gamma_{TE} = 2(n_g^2 - n_0^2)\left(\frac{\pi d}{\lambda_0}\right)^2 \tag{18}$$

and for TM polarization,

$$\Gamma_{TM} = 2\left(\frac{n_0}{n_g}\right)^2 (n_g^2 - n_0^2)\left(\frac{\pi d}{\lambda_0}\right)^2 \tag{19}$$

where n_0 is the refractive index of the substrate, n_g is the refractive index of the waveguide region, and λ_0 is the wavelength of radiation in free space. For a large d/λ_0, the optical confinement factors can be calculated numerically by solving transcendental equations.

We have also measured LD amplified spontaneous emission spectra for drive currents below threshold. The facet light of the LD comes from multiply reflected amplified spontaneous emission in the laser cavity and can be modeled using (16) multiplied by a factor accounting for such reflections from the LD facets [24].

III. Theoretical Results and Comparison with Experiment

In this section, we compare our theoretical results with experimental data using an index guided $In_{1-x}Ga_xAs_yP_{1-y}$ waveguide structure fabricated on an InP substrate. The bandgap wavelength is λ_g = 1.28 μm in the active region at 295 K. Most material parameters are taken from [32]–[34]. The lattice-matching relation between x and y for the $In_{1-x}Ga_xAs_yP_{1-y}$/InP system is

$$x = 0.1894y/(0.4184 - 0.013y). \tag{20}$$

The energy equivalent interband momentum matrix E_p is linearly interpolated from those of the InAs, GaAs, InP,

and GaP materials [35]. The spin-orbit split-off energy is given by

$$\Delta = 0.114 + 0.26y - 0.02y^2. \tag{21}$$

The effective masses for electrons m_e^*, heavy holes m_{hh}^*, and light holes m_{lh}^* are

$$m_e^* = 0.08 - 0.039y$$

$$m_{hh}^* = 0.45$$

and

$$m_{lh}^* = 0.12 - 0.069y. \tag{22}$$

The band-gap energy as a function of temperature is given by [32]

$$E_g^0(T) = E_g^0(0) - \frac{\alpha T^2}{\beta + T}\,(\text{eV}) \tag{23}$$

where $\alpha = 0.426 \times 10^{-3}$, $\beta = 224$, and $E_g^0(0)$ is determined from $E_g^0(295\text{ K}) = 1.35 - 0.775y + 0.149y^2$ (eV). For our material, we have $x = 0.25$, $y = 0.55$, and $E_g^0(0) = 1.0398$ eV. The refractive index n_g in the $In_{1-x}Ga_xAs_yP_{1-y}$ active region is taken to be 3.435 and the substrate refractive index n_0 is 3.20 [32].

In Fig. 3, we show experimental data (top figure) for the ratio of facet light with TE polarization and window light together with theoretical results (bottom figure) for the LED at 25°C. The zero of the experimental data has been adjusted since there should be no gain far below the bandgap. The vertical scale is in arbitrary units. From the overall fit of the spectrum, we extract the carrier density for five drive currents, $I = 50$, 20, 10, 5 and 2 mA. The same parameters are used to fit the TM polarization data at 25°C in Fig. 4. The differences between the TE and TM results are mainly due to the optical confinement factor, which enters the modal gain in the expression for facet light. Using the same model, we also compare experimental data at 55°C for both polarizations in Figs. 5 and 6. Overall the agreement between experiment and calculation is very good. We can see that at the same injection current, the amplified spontaneous emission spectrum reduces in magnitude and shifts toward lower energies when temperature is increased.

In Fig. 7, we plot the difference in chemical potential for electrons and holes at 25 and 55°C as a function of carrier density. Since this is the optical transparency energy in the gain spectrum, or the zero crossing point in the $\ln(L^F/L^W)$ spectrum, it provides a good estimation of the carrier density for spectra such as those in Figs. 3 and 4. Theoretical results which do not include conduction band nonparabolicity are also shown as dashed curves in Fig. 7. As may be seen, there is an overestimation of quasi-Fermi level using a parabolic band model which can range from a few meV to 30 meV depending on the carrier concentration. In Fig. 8(a), we compare our theoretical gain spectra with (solid curve) and without (dashed curve) the conduction band nonparabolicity effects at a carrier concentration of $n = 1.7 \times 10^{18}/\text{cm}^3$. Fig. 8(a) shows that a consequence of using the parabolic band model [dashed lines in Figs. 7 and 8(a)] is that the transparency

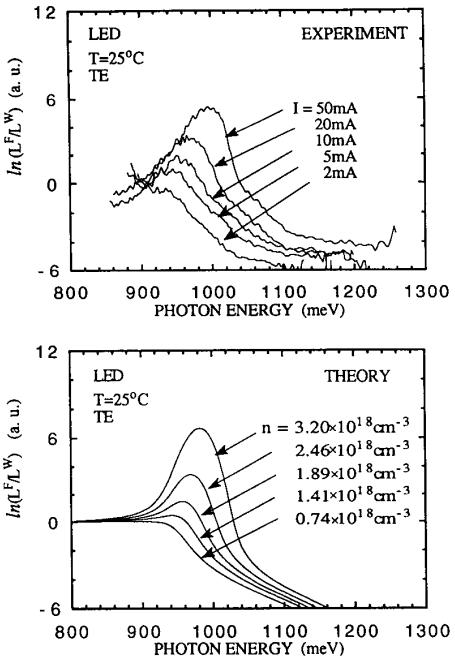

Fig. 3. Spectrum of the ratio of facet light to window light of the LED at $T = 25$°C at $I = 50$, 20, 10, 5, and 2 mA for TE polarization. The upper figure shows the experimental data and the lower figure shows our theoretical results, both with arbitrary vertical scale. The corresponding carrier density is indicated in the lower figure.

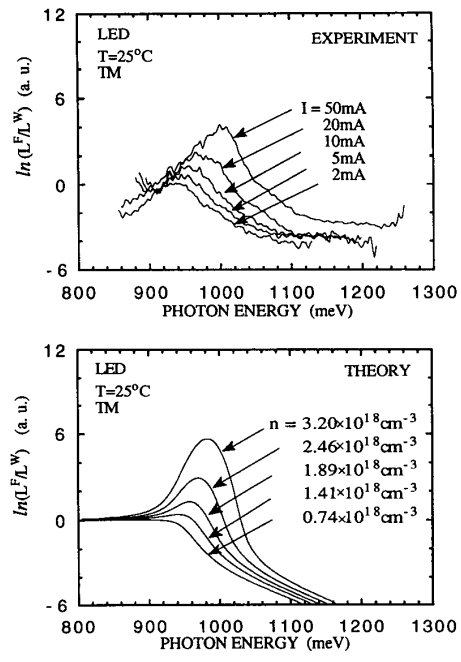

Fig. 4. Same as Fig. 3, except for TM polarization.

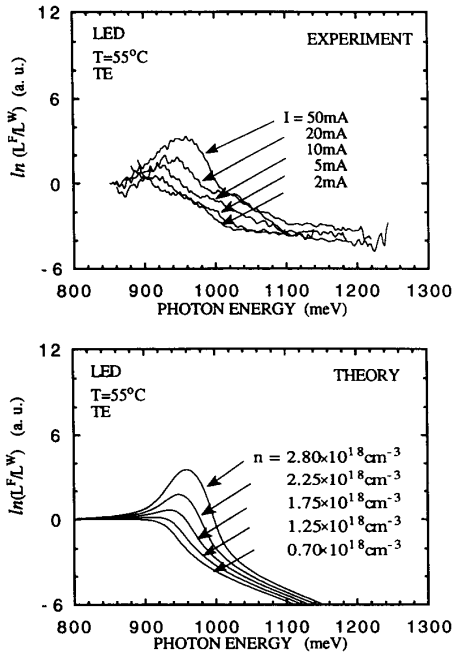

Fig. 5. Spectrum of the ratio of facet light to window light of the LED at $T = 55°C$ at $I = 50$, 20, 10, 5, and 2 mA for TE polarization. The upper figure shows the experimental data and the lower figure shows our theoretical results, both with arbitrary vertical scale. The corresponding carrier density is indicated in the lower figure.

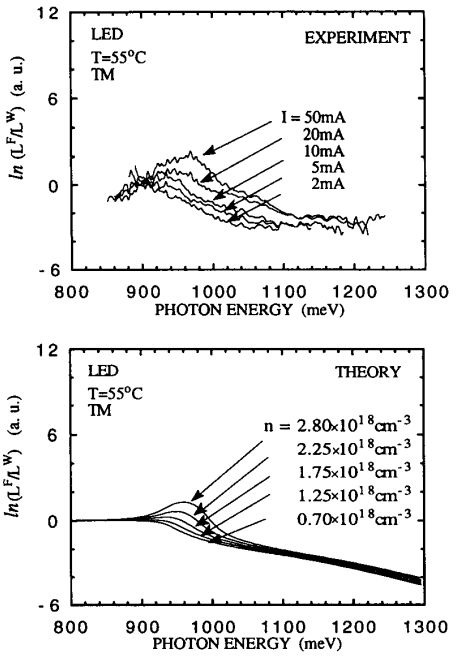

Fig. 6. Same as Fig. 5, except for TM polarization.

energy in the gain spectrum has a significant blue shift. In Fig. 8(b), we compare calculated gain using (7) (solid curve) and the conventional model, (4) (dashed line). Both

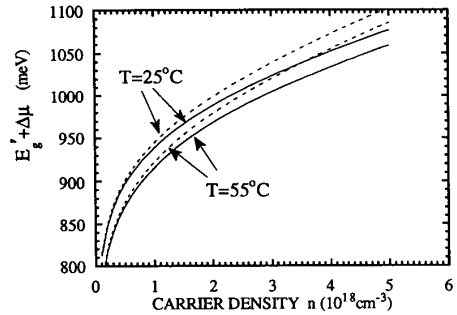

Fig. 7. Separation of electron and hole chemical potential as a function of the carrier density at $T = 25°C$ and 55°C with (solid curves) and without (dashed curves) conduction band nonparabolicity.

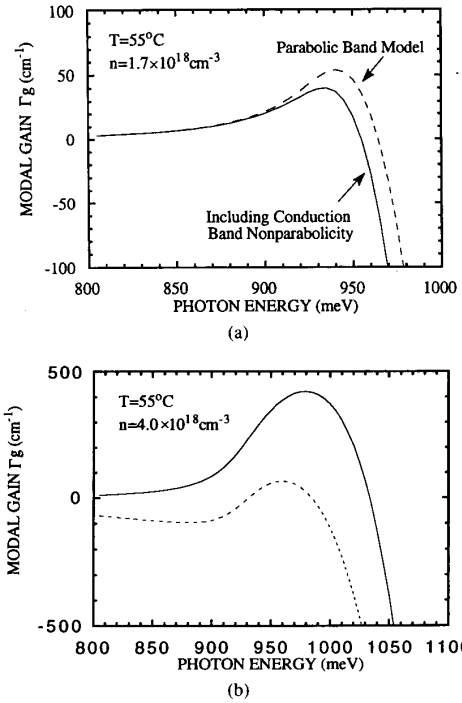

Fig. 8. (a) The modal gain spectrum calculated with (solid curve) and without (dashed curve) conduction band nonparabolicity at $T = 55°C$, a carrier concentration $n = 1.7 \times 10^{18}/cm^3$, and $\gamma_k = 25$ meV. (b) Comparison of calculated gain using (7) (solid curve) and conventional model, (4) (dashed line). Both models include conduction band nonparabolicity $\gamma_k = 25$ meV, $T = 55°C$, and $n = 4.0 \times 10^{18}/cm^3$.

models include conduction band nonparabolicity, $\gamma_k = 25$ meV, and carrier density is $4.0 \times 10^{18}/cm^3$. It is clear from this figure that the transparency energy in the conventional model does not occur at $\Delta\mu$. In addition, the conventional gain model predicts lower peak gain and absorption below the band edge.

In Fig. 9, we show a comparison of calculated gain spectra with experimental data for the LD at $T = 55°C$ for three injection currents, $I = 20$, 15, and 10 mA, which are all below lasing threshold, $I_{th} = 21.5$ mA. The overall fit is good. The experimental gain spectra were measured

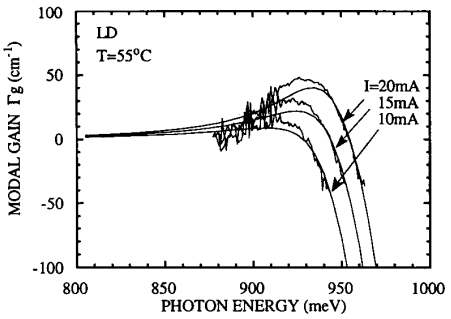

Fig. 9. Comparison of the theoretical gain spectra (smooth lines) and the experimental data (lines with noise) at three current levels I = 20, 15, and 10 mA (n = 1.7 × 10^{18}/cm^3, 1.48 × 10^{18}/cm^3, and 1.20 × 10^{18}/cm^3, respectively) at T = 55°C. γ_k = 25 meV. The experimental gain spectra were measured using the Hakki-Paoli method. A background free carrier absorption of 21/cm is found for this set of data.

using the Hakki-Paoli or Fabry-Perot transmission modulation technique [36], [37]. This fitting procedure also provides a method to extract carrier concentration for the LD. In addition, the transparency energies, or the zero crossing of the gain spectrum, were measured independently using the experimental method of [38], and the results agree very well with the data shown in Fig. 9. The fast decaying behavior of the experimental data at the low energy side can be improved using the phenomenological line shape model discussed in [39] and [40]. A *rigorous* theoretical basis for such a line shape has yet to be established. From the photon energy (935 meV) of the peak theoretical gain for I = 20 mA and T = 55°C, we obtain a wavelength 1.326 μm, which is close to the measured lasing wavelength of the LD, λ = 1.321 μm. Similarly, our theory gives a peak wavelength of the gain at λ = 1.312 μm for T = 25°C and I = 10 mA, which agrees very well with the experimental value λ = 1.310 μm.

In Fig. 10(a) and (b), we plot carrier density as a function of injection current for both LED and LD at two temperatures. The data for the LED are obtained from Figs. 3-6, and some of the data for the LD are obtained from Fig. 9 with the remainder from similar measurements. It is apparent from the data that carrier pinning in the LED is less substantial and less temperature sensitive than in the LD. We note that the presence of two mirrors which form the cavity of a Fabry-Perot laser create definite longitudinal resonances called cavity modes. The formal analogy which exists between a Landau-Ginzburg phase transition and photon statistics around laser threshold [4]-[6] allows us to describe all photons in cavity modes below threshold as (unsustainable) fluctuations. Hence, within this formalism, the extra subthreshold photon intensity in a laser diode arises from cavity mode photon fluctuations and it is these photon fluctuations that cause carrier density to be pinned more effectively than in the corresponding LED. To some extent, the standard rate equations deal with an aspect of this issue by adopting a mean-field approach. However, to understand the carrier pinning due to photon fluctuations into cavity modes we

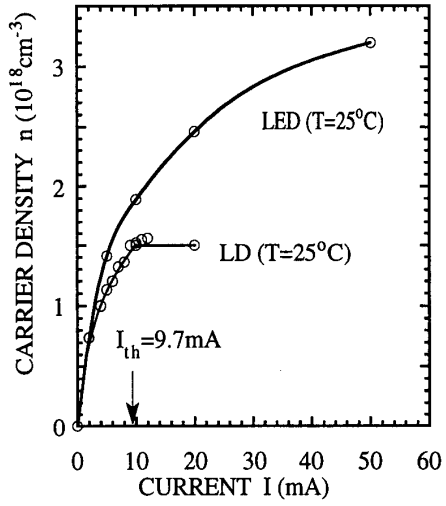

Fig. 10. Carrier density versus injection current plotted for both LED and LD at (a) T = 25°C and (b) T = 55°C. Some of the circles are obtained from the fit in Figs. 2-5 for LED and Fig. 8 for LD. The solid curves are just a visual guide.

must consider the possible recombination channels in both the LD and the LED.

Since the only difference between the LED and LD is the presence of cavity modes in the LD, it is clear that fluctuations into cavity modes account for approximately half the current flowing into the LD at threshold. To reach threshold it is necessary to supply an extra current to overcome the effects of this carrier pinning. The remaining current is due to recombination processes present in both the LED and LD. At T = 25°C, the threshold current for the LD is I_{th} = 9.7 mA. The contribution to this current from photons fluctuating into cavity modes is approximately 4 mA. The threshold current for the LD at T = 55°C is I_{th} = 21.5 mA and the contribution of photon fluctuations is now 10 mA. The importance of optical

mode fluctuations is clearly enhanced at elevated temperatures. Such subthreshold fluctuations act as a feedback mechanism which causes laser threshold *current* to increase with increasing temperature. On the other hand, the variation of *carrier density* at threshold in the LD remains relatively temperature insensitive ($n_{th}(T = 25°C) = 1.5 \times 10^{18}/cm^3$ and $n_{th}(T = 55°C) = 1.75 \times 10^{18}/cm^3$) and is similar to that expected for a simple $(T + 273)^{3/2}$ power law behavior.

The temperature dependence of LED *current at the laser threshold carrier density* has both radiative and nonradiative components. The radiative channels are single pass ASE and spontaneous emission. The nonradiative carrier and photon recombination channels may have contributions from the possible presence of defects, weakly temperature-dependent Auger recombination [41] and free-carrier absorption. Clearly, the current required for the LED to attain the same carrier density as the laser at threshold will also contribute to the overall temperature sensitivity of LD threshold current.

IV. Conclusion

In summary, we have investigated the temperature dependence of amplified spontaneous emission spectra in LED's and gain spectra in LD's of the same geometry. We show that our theoretical model, which makes use of a relationship between gain and spontaneous emission, can explain the experimental data very well. Using this model, carrier pinning in a laser diode and its temperature dependence has been investigated. We conclude that photons fluctuating into cavity modes of a laser diode at subthreshold drive current contribute to the temperature dependence of the device.

If, in the future, it is possible to suppress photon cavity mode fluctuations then it might be realistic to expect a reduction in the temperature sensitivity of laser diode threshold current. One approach might be to use microdisk lasers [42], [43] in which only one optical mode overlaps the gain spectrum.

Acknowledgment

We thank E. J. Flynn for providing the devices used in this paper and K. Wecht for antireflection coating the laser diodes. Part of this work was performed when S. L. Chuang was visiting AT&T Bell Laboratories.

References

[1] Y. Horikoshi, "Temperature dependence of laser threshold current," in *GaInAsP Alloy Semiconductors*, T. P. Pearsall, Ed. New York: Wiley, 1982, pp. 379-411.

[2] A. R. Adams, M. Asada, Y. Suematsu, and S. Arai, "The temperature dependence of the efficiency and threshold current of InGaAsP lasers related to intervalence band absorption," *Japan. J. Appl. Phys.*, vol. 19, pp. L621-624, 1980.

[3] N. Holonyak, Jr., R. M. Kolbas, R. D. Dupuis, and P. D. Dapkus, "Quantum-well heterostructure lasers," *IEEE J. Quantum Electron.*, vol. QE-16, pp. 170-186, 1980.

[4] J. O'Gorman, A. F. J. Levi, S. Schmitt-Rink, T. Tanbun-Ek, D. L. Coblentz, and R. A. Logan, "On the temperature sensitivity of semiconductor lasers," *Appl. Phys. Lett.*, vol. 60, pp. 157-159, 1992.

[5] J. O'Gorman, A. F. J. Levi, T. Tanbun-Ek, D. L. Coblentz, and R. A. Logan, "Temperature dependence of long wavelength semiconductor lasers," *Appl. Phys. Lett.*, vol. 60, pp. 1058-1060, 1992.

[6] A. F. J. Levi, J. O'Gorman, S. Schmitt-Rink, T. Tanbun-Ek, D. L. Coblentz, and R. A. Logan, "Temperature dependence of semiconductor lasers," in *Proc. SPIE*, Physics and Simulation of Optoelectronic Devices, vol. 1679, pp. 85-95, 1992.

[7] Y. Zou, J. S. Osinski, P. Grodzinski, P. D. Dapkus, W. Rideout, W. F. Sharfin, and F. D. Crawford, "The effect of Auger recombination and differential gain on the temperature sensitivity of 1.5 μm quantum well lasers," *Appl. Phys. Lett.*, vol. 62, pp. 175-177, 1993.

[8] M. Yamada and Y. Suematsu, "Analysis of gain suppression in undoped injection lasers," *Japan. J. Appl. Phys.*, vol. 52, pp. 2653-2664, 1981.

[9] F. Stern, "Semiconductor lasers: theory," in *Laser Handbook*, F. T. Arecchi and E. O. Schulz-Dubois, Eds. Amsterdam: North-Holland, 1972.

[10] C. J. Hwang, "properties of spontaneous and stimulated emission in GaAs junction lasers. I. Densities of states in the active regions," *Phys. Rev. B*, vol. 2, pp. 4117-4125, 1970; and "II. Temperature dependence of threshold current and excitation dependence of superradiances spectra," *Phys. Rev. B*, vol. 2, pp. 4126-4134, 1970.

[11] M. Asada, A. Kameyama, and Y. Suematsu, "Gain and intervalence band absorption in quantum-well lasers," *IEEE J. Quantum Electron.*, vol. QE-20, pp. 745-753, 1984.

[12] D. Ahn, S. L. Chuang, and Y. C. Chang, "Valence-band mixing effects on the gain and the refractive index change of quantum-well lasers," *J. Appl. Phys.*, vol. 64, pp. 4056-4064, 1988.

[13] D. Ahn and S. L. Chuang, "Optical gain in a strained-layer quantum-well laser," *IEEE J. Quantum Electron.*, vol. 24, pp. 2400-2406, 1988.

[14] ——, "Optical gain and gain suppression of quantum-well lasers with valence band mixing," *IEEE J. Quantum Electron.*, vol. 26, pp. 13-24, 1990.

[15] S. Schmitt-Rink, C. Ell, and H. Haug, "Many-body effects in the absorption, gain, and luminescence spectra of semiconductor quantum-well structures," *Phys. Rev. B*, vol. 33, pp. 1183-1189, 1986.

[16] M. F. Pereira, Jr., S. W. Koch, and W. W. Chow, "Many-body effects in the gain spectra of strained quantum wells," *Appl. Phys. Lett.*, vol. 59, pp. 2941-2943, 1991.

[17] C. Ell and H. Haug, "Absorption and optical gain spectra and band gap renormalization of highly excited quantum well systems," *Phys. Stat. Sol. (b)*, vol. 159, pp. 117-124, 1990.

[18] H. Haug and D. B. Tran Thoai, "Gain spectrum of an e-h liquid in direct gap semiconductors," *Phys. Stat. Sol. (b)*, vol. 98, pp. 581-589, 1980.

[19] H. Haug and S. Schmitt-Rink, "Electron theory of the optical properties of laser-excited semiconductors," *Prog. Quantum Electron.*, vol. 9, pp. 3-100, 1984. (see p. 13)

[20] M. Yamanishi and Y. Lee, "Phase dampings of optical dipole moments and gain spectra in semiconductor lasers," *IEEE J. Quantum Electron.*, vol. QE-23, pp. 367-370, 1987.

[21] A. I. Kucharska and D. J. Robbins, "Lifetime broadening in GaAs-AlGaAs quantum well lasers," *IEEE J. Quantum Electron.*, vol. 26, pp. 443-448, 1990.

[22] J. O'Gorman, S. L. Chuang, and A. F. J. Levi, "Carrier pinning by mode fluctuations in laser diodes," *Appl. Phys. Lett.*, vol. 62, pp. 1454-1456, 1993.

[23] E. O. Göbel, "Photoluminescence and optical gain of GaInAsP," in *GaInAsP Alloy Semiconductors*, T. P. Pearsall, Ed. New York: Wiley, 1982, pp. 379-411.

[24] B. Zee, "Broadening mechanism in semiconductor (GaAs) lasers: Limitations to single mode power emission," *IEEE J. Quantum Electron.*, vol. QE-14, pp. 727-736, 1978.

[25] G. Fuchs, J. Horer, A. Hangleiter, V. Harle, F. Scholz, R. W. Glew, and L. Goldstein, "Intervalence band absorption in strained and unstrained InGaAs multiple quantum well structures," *Appl. Phys. Lett.*, vol. 60, pp. 231-233, 1992.

[26] E. O. Kane, "Band structure of indium antimonide," *J. Phys. Chem. Solid*, vol. 1, pp. 249-261, 1957.

[27] G. Lasher and F. Stern, "Spontaneous and stimulated recombination radiation in semiconductors," *Phys. Rev.*, vol. 133, pp. A553-A563, 1964.

[28] J. Lee and M. O. Vassell, "The small-signal response of 1.5 μm

multiple-quantum-well lasers in a two-band-model approximation," *IEEE J. Quantum Electron.*, vol. 28, pp. 624-634, 1992.
[29] H. C. Casey, Jr., and M. B. Panish, *Heterostructure Lasers, Part A: Fundamental Principles*. New York: Academic, 1978.
[30] B. Sermage, D. S. Chemla, D. Sivco, and A. Y. Cho, "Comparison of Auger recombination in GaInAs-AlInAs multiple quantum well structure and in bulk GaInAs," *IEEE J. Quantum Electron.*, vol. QE-22, pp. 774-780, 1986.
[31] J. I. Pankove, *Optical Processes in Semiconductors*. New York: Dover, 1971.
[32] S. Adachi, Ed., *Properties of Indium Phosphide*. London: INSPEC, IEE, 1991.
[33] Landolt-Bornstein, *Numerical Data and Functional Relationships in Science and Technology*, K. H. Hellwege, Ed. Berlin: Springer, New series, Group III, vol. 17a, 1982; Group III-V, vol. 22a, 1986.
[34] S. L. Chuang, "Efficient band-structure calculations of strained quantum wells," *Phys. Rev. B*, vol. 43, pp. 9649-9661, 1991.
[35] P. Lawaetz, "Valence-band parameters in cubic semiconductors," *Phys. Rev. B*, vol. 4, pp. 3460-3467, 1971.
[36] B. W. Hakki and T. L. Paoli, "Gain spectra in GaAs double-heterostructure injection lasers," *J. Appl. Phys.*, vol. 46, pp. 1299-1306, 1975.
[37] I. P. Kaminow, G. Eisentein, and L. W. Stulz, "Measurement of the modal reflectivity of an antireflection coating on a superluminescent diode," *IEEE J. Quantum Electron.*, vol. QE-19, pp. 493-495, 1983.
[38] P. A. Andrekson, N. A. Olsson, T. Tanbun-Ek, R. A. Logan, D. Coblentz, and H. Temkin, *Electron. Lett.*, vol. 28, p. 171, 1992.
[39] M. P. Kesler and C. Harder, "Spontaneous emission and gain in GaAlAs quantum well lasers," *IEEE J. Quantum Electron.*, vol. 27, pp. 1812-1816, 1991.
[40] M. Asada, "Intraband relaxation time in quantum-well lasers," *IEEE J. Quantum Electron.*, vol. 25, pp. 2019-2026, 1989.
[41] G. Fuchs, C. Schiedel, A. Hangleiter, V. Harle, and F. Scholz, "Auger recombination in strained and unstrained InGaAs/InGaAsP multiple quantum-well lasers," *Appl. Phys. Lett.*, vol. 62, pp. 396-398, 1993.
[42] S. L. McCall, A. F. J. Levi, R. E. Slusher, S. J. Pearton, and R. A. Logan, "Whispering-gallery mode microdisk lasers," *Appl. Phys. Lett.*, vol. 60, p. 289, 1992.
[43] A. F. J. Levi, R. E. Slusher, S. L. McCall, T. Tanbun-Ek, D. L. Coblentz, and S. J. Pearton, "Room temperature operation of microdisk lasers with sub-milliamp threshold current," *Electron. Lett.*, vol. 28, p. 1010, 1992.

Shun Lien Chuang (S'78-M'82-SM'88) was born in Taiwan in 1954. He received the B.S. degree in electrical engineering from the National Taiwan University in 1976 and the M.S., E.E., and Ph.D. degrees in electrical engineering from the Massachusetts Institute of Technology, Cambridge, in 1980, 1981, and 1983, respectively.

While in graduate school, he held research and teaching assistantships, and also served as a recitation instructor. He is currently an Associate Professor and will be a Full Professor in August, 1993 with the Department of Electrical and Computer Engineering, University of Illinois, Urbana. He is conducting research in semiconductor lasers, quantum-well optoelectronic devices, nonlinear optics, and fiber optics. He recently developed a graduate course on integrated optics and optoelectronics. He has been cited several times for Excellence in Teaching at the University of Illinois. In 1989 he was a resident visitor at AT&T Bell Laboratories, Holmdel, NJ, conducting research on high speed quantum-well physics and devices in the Department of Photonics Switching Device Research. He was also a consultant at Bellcore, Red Bank, NJ in 1990; and at Polaroid, Boston, MA, in 1991. He has published more than 130 journal and conference papers.

Dr. Chuang is a member of the Optical Society of America, the American Physical Society, and URSI commissions B and D. He will be a co-Editor for a special issue on Terahertz generation, physics and applications in the *Journal of Optical Society America, B.*

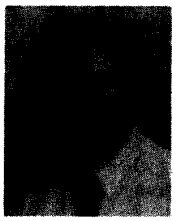

James O'Gorman was born in Tralee, Co Kerry, Ireland, on September 25, 1959. He received the B.Sc. degree in physics, mathematical physics, and mathematics and a Diploma in computer science from University College Dublin in 1979 and 1980, respectively. In 1984 he received the Grad. Inst. P. (First Class) from the Institute of Physics (London). In 1989 he received the Ph.D. degree in physics from the University of Dublin, Trinity College, Dublin. His doctoral thesis concerned nonlinear dynamics of external cavity injection lasers.

From 1979 to 1989 he was employed as a physics teacher in the Dublin Institute of Technology. From 1990 to 1992 he was a post-Doctoral Member of the Technical Staff at AT&T Bell Laboratories, Murray Hill, NJ. While at Bell Laboratories his research mainly concerned voltage controlled intracavity loss modulated lasers, high-power ultrashort pulse generation with laser diodes, cavity formation in semiconductor injection lasers, and the temperature dependence of long wavelength semiconductor lasers. Since October 1992 he has been a Research Fellow with Optronics Ireland, Trinity College, Dublin. His research interests include the physics of semiconductor injection lasers, the effect of quantum size on physical properties of semiconductors, ultrashort pulse generation with laser diodes, and optical bistability in laser diode amplifiers.

Dr. O'Gorman is a member of the Optical Society of America.

A. F. J. Levi, photograph and biography not available at the time of publication.